

## Supplemental material for “Medium-enhanced $c\bar{c}$ radiation”

Maximilian Attems,<sup>1,\*</sup> Jasmine Brewer,<sup>1,†</sup> Gian Michele Innocenti,<sup>2,‡</sup> Aleksas Mazeliauskas,<sup>1,§</sup>  
Sohyun Park,<sup>1,¶</sup> Wilke van der Schee,<sup>1,\*\*</sup> Gregory Soyez,<sup>3,††</sup> and Urs Achim Wiedemann<sup>1,‡‡</sup>

<sup>1</sup>*Theoretical Physics Department, CERN, 1211 Geneva 23, Switzerland*

<sup>2</sup>*Experimental Physics Department, CERN, 1211 Geneva 23, Switzerland*

<sup>3</sup>*IPhT, Université Paris-Saclay, CNRS UMR 3681, CEA Saclay, F-91191 Gif-sur-Yvette, France*

Here, we describe in more detail the two Monte Carlo implementations of medium-modified parton showers, used in the main text.

**Heavy quark production in JetMed.** JetMed implements a medium-modified parton shower based on a factorized picture of vacuum-like and medium-induced parton splittings. The vacuum evolution is correct at single logarithmic accuracy in the strongly ordered collinear limit [1–4]. It is supplemented by medium-modifications as follows:

1. Vacuum emissions are generated by an angular-ordered shower starting from  $\theta_{\max} = 1$ , with a minimal transverse momentum cut-off  $k_{\perp,\min} = 0.25$  GeV. In the region  $k_{\perp}^3 \theta < 2\hat{q}$ , medium-induced emissions are dominant and vacuum emissions are hence vetoed. Furthermore, emission with  $\theta < \theta_c = 2/\sqrt{\hat{q}L^3}$  lose energy coherently with their emitter and can be treated as if they were happening outside the medium (see step 3 below).
2. Medium-induced emissions are generated for each parton produced in the first step. The collinear splittings are ordered in an emission time  $0 < t < L$  and computed with multiple-soft splitting kernels [5]. For  $g \rightarrow gg$  splitting the formation time is given by

$$t_f = \sqrt{\frac{2z(1-z)xE}{\hat{q}(1-z(1-z))}} \quad (1)$$

and the splitting rate is

$$\frac{d^2\Gamma_{\text{med}}}{dzdt} = \frac{\alpha_s P_{a \rightarrow bc}^{\text{vac}}(z)}{\sqrt{2\pi}} \frac{1}{t_f}. \quad (2)$$

The coupling constant  $\alpha_s$  is a fixed model parameter without scale evolution. Partons produced both from vacuum-like and medium-induced splittings acquire an average transverse momentum

$$\langle k_{\perp}^2 \rangle(t, t_0) = \int_{t_0}^t dt' \hat{q}(t') \quad (3)$$

while traversing the medium. The acquired transverse momentum is sampled from a gaussian distribution and added to the parton transverse momentum (which is zero for medium-induced emissions). Emissions at angles larger than  $\theta_{\max}$  are discarded.

3. For each parton that leaves the medium after step 2, vacuum-like emissions outside the medium are restarted with  $\theta_{\max}$ . That the first emission outside the medium does not obey angular ordering is a consequence of the loss of coherence in the medium. Emissions with  $k_{\perp}\theta > 2/L$  or  $\theta > \theta_c$  are vetoed.

The generated partons can then be passed to **FastJet** to construct infrared and collinear safe observables. By default, we consider  $R = 0.4$  anti- $k_{\perp}$  jets.

To include charm mass effects, we have supplemented the JetMed evolution as follows. To logarithmic accuracy, the vacuum splitting functions  $g \rightarrow q\bar{q}$  are the same for charm quarks and massless quarks, but charm quarks have to pass the mass threshold. This is implemented by vetoing  $g \rightarrow c\bar{c}$  if the generated transverse momentum does not satisfy  $k_{\perp}^2 > m_c^2$ . For medium-induced  $g \rightarrow c\bar{c}$ , the multiple-soft splitting kernel is the  $\kappa$ -integrated version of Eq. 3 in the main text to leading logarithmic accuracy. The pair is produced collinearly and it acquires transverse momentum in the medium as explained below Eq. (3). In analogy to the vacuum case, the medium-induced splitting is vetoed if the medium-induced momentum transfer is insufficient to lift the  $c\bar{c}$ -pair above the mass threshold  $k_{\perp}^2 > m_c^2$ . In addition, gluon radiation from a heavy quark is vetoed within the dead cone angle  $m_Q/E$  [6]. This procedure implements mass effects to leading logarithmic accuracy in the vacuum parton shower and treats the medium-induced  $g \rightarrow c\bar{c}$  splitting on equal footing with other medium-induced splittings in JetMed.

**Simple dipole-shower.** To further establish the robustness of our main conclusions to model assumptions, we additionally provide results for a simple dipole shower supplemented with medium-modified splitting functions. We follow the public implementation of a massless  $\kappa$ -ordered dipole shower with final-state radiation only [7, 8]. The shower is initialized with a color neutral  $q\bar{q}$  or  $gg$  pair of momenta

$$p_1^{\mu} = E(1, 0, 1, 0), \quad p_2^{\mu} = E(1, 0, -1, 0), \quad (4)$$

and it is evolved in  $t = \kappa^2$  from the initial scale  $E^2$  down to the cut-off scale  $t_0 = 1 \text{ GeV}^2$ . Gluons and  $N_f = 5$  massless quark flavor are included in the evolution. For the medium modification, the  $q \rightarrow qg$ ,  $g \rightarrow gg$  and (massless)  $g \rightarrow q\bar{q}$  vacuum splitting functions are supplemented with additive BDMPS-Z corrections  $P_{a \rightarrow bc}^{\text{tot}} = P_{a \rightarrow bc}^{\text{vac}} + P_{a \rightarrow bc}^{\text{med}}$ . For reasons of technical

simplicity, we use for all splitting functions the small- $z$  limit

$$P_{a \rightarrow bc}^{\text{med}}(E, \kappa^2, z) \Big|_{z \ll 1} = P_{a \rightarrow bc}^{\text{vac}}(z) \mathfrak{J} \left( \frac{\kappa^2}{\hat{q}_c L}, \frac{zE}{\frac{1}{2} \hat{q}_c L^2} \right) \Big|_{z \ll 1}. \quad (5)$$

Here,  $\mathfrak{J}$  is the universal modification factor

$$\mathfrak{J}(\tilde{\kappa}^2, \tilde{\omega}) = \frac{\kappa^2}{2\omega^2} \Re \int_0^L dt \int_t^\infty d\bar{t} \int d\mathbf{r} e^{-\epsilon|t| - \epsilon|\bar{t}|} \times e^{-\frac{1}{4} \int_t^\infty d\xi \hat{q}(\xi) \mathbf{r}^2} e^{-i \kappa \cdot \mathbf{r}} \frac{\partial}{\partial \mathbf{x}} \cdot \frac{\partial}{\partial \mathbf{r}} \mathcal{K}[\mathbf{x} = 0, t; \mathbf{r}, \bar{t}], \quad (6)$$

which depends on the rescaled variables  $\tilde{\kappa}^2 \equiv \frac{\kappa^2}{\hat{q}_c L}$  and  $\tilde{\omega} \equiv \frac{\omega}{\frac{1}{2} \hat{q}_c L^2}$  with  $\omega = zE$ . The variable  $z$  denotes the momentum fraction of the softer splittee, which is the gluon for  $q \rightarrow qg$  and  $g \rightarrow gg$  and the quark or anti-quark for  $g \rightarrow q\bar{q}$ . Correspondingly,  $\hat{q}_c = \hat{q}_A = C_A \hat{q}$  for  $q \rightarrow qg$ ,  $g \rightarrow gg$  and  $\hat{q}_c = C_F \hat{q}$  for  $g \rightarrow q\bar{q}$ .

For the  $g \rightarrow gg$  and  $q \rightarrow qg$  splitting functions, medium modifications of the form Eq. (5) have been implemented previously in the Q-PYTHIA medium-modified parton shower [9]. Our simple dipole-shower parallels this logic but includes  $g \rightarrow q\bar{q}$ .

**Supplementary results for the simple medium-modified dipole shower.** For each event we reconstruct anti- $k_t$  jets with  $R = 0.4$ . We define  $q\bar{q}$ -tagged jets as jets containing a single  $q\bar{q}$  pair that originates from the same gluon splitting. To simulate the fraction  $N^{q\bar{q}}/N^{\text{inc}}/N_f$  of the number of  $q\bar{q}$ -tagged over inclusive jets of specific flavor, we require additional information about the hard production rate of partons  $i$  (quark or gluon) with initial energy  $E$ . For the relevant partonic cross-sections  $d\sigma_i/dE$  we use leading order results averaged over rapidity window  $y < 1$  at  $\sqrt{s} = 5.02$  TeV from Ref. [10] and we take  $E = p_T$ . The jet  $p_T$  spectra are then given by weighting average contributions from single initial parton jets with the respective leading-order partonic cross-section

$$\frac{d\sigma_j}{dp_T} = \int dE \left( \frac{d\sigma_g}{dE} \frac{dN_{g \rightarrow j}(E)}{dp_T} + \frac{d\sigma_q}{dE} \frac{dN_{q \rightarrow j}(E)}{dp_T} \right). \quad (7)$$

For the ratio  $N^{q\bar{q}}/N^{\text{inc}}/N_f$  of  $q\bar{q}$ -tagged over inclusive jets, this modeling leads to a vacuum baseline shown in Fig. 1.

In comparison to the vacuum baseline obtained from **JetMed** (see the blue line in Fig. ??(b)), the vacuum baseline of the ratio of  $q\bar{q}$ -tagged over inclusive jets shown here is a factor 1.2 (1.1) larger for  $p_T = 200$  (100) GeV jets. In the region of  $p_T = 20 - 50$  GeV, deviations between the baselines of **JetMed** and this simple dipole shower grow larger than a factor 2. We note in this context that a dipole-shower and an angular-ordered shower agree only up to leading logarithmic accuracy. Also, the effect of charm mass is beyond leading logarithmic accuracy and it is included in **JetMed** but not in this simple

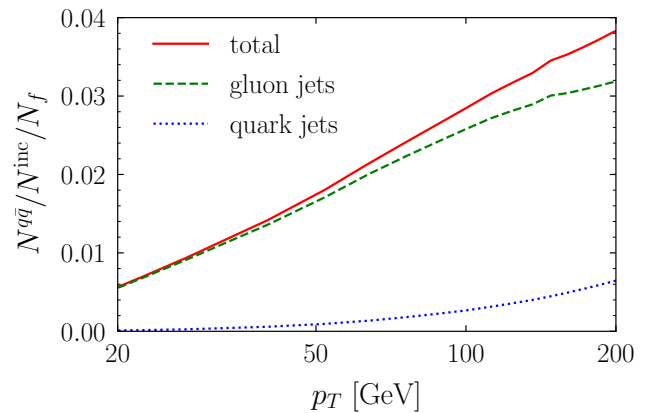


FIG. 1. The yield of  $q\bar{q}$ -tagged  $R = 0.4$  jets per flavor as a fraction of all jets, calculated from the simple stand-alone dipole vacuum parton shower supplemented with Eq. (7).

dipole shower. In general, contributions beyond leading logarithmic accuracy can grow large if the phase space for parton splitting becomes small which is the case for low  $p_T < 50$  GeV. Taking this into account, we conclude that the vacuum baselines of **JetMed** and of this simple dipole-shower agree within expected uncertainties.

We show the nuclear modification factor  $R_{AA}$  in this simulation for inclusive and for  $q\bar{q}$ -tagged jets in Fig. 2(a). If the medium modification of all splitting functions is included, then  $R_{AA}^{\text{inc}}$  for inclusive jets shows the significant suppression characteristic of jet quenching (purple solid). The  $R_{AA}^{q\bar{q}}$  for  $q\bar{q}$ -tagged jets shows a significantly smaller suppression (purple hatched) since the effects leading to jet quenching in  $R_{AA}^{\text{inc}}$  are partially compensated by a characteristic rate enhancement due to medium-modified  $g \rightarrow q\bar{q}$ . If only the  $g \rightarrow q\bar{q}$  splitting function is medium-modified, there is little modification of inclusive jets (solid orange) but substantial enhancement of  $q\bar{q}$ -tagged jets (hatched orange). In Fig. 2(b) we show the double ratio  $R_{AA}^{q\bar{q}}/R_{AA}^{\text{inc}}$ , which helps to isolate the effects from medium-enhanced  $q\bar{q}$  production. Irrespective of whether the parton shower includes medium modifications to all splitting functions (purple band) or only modifications to the  $g \rightarrow q\bar{q}$  splitting function (orange band), a significant enhancement of the double ratio is observed. This signals the dominant role of medium-enhanced  $g \rightarrow q\bar{q}$  splitting in this enhancement.

In both panels of Fig. 2 we additionally show in green the results of the reweighting procedure applied to this parton shower. The reweighting is in reasonable agreement with the effect of enhancing only the  $g \rightarrow c\bar{c}$  splitting.

Fig. 2 corroborates our main conclusions in several ways. First, within the bands of  $\hat{q}L$  variation, the enhancement of  $R_{AA}^{q\bar{q}}/R_{AA}^{\text{inc}}$  obtained from the medium-modified dipole parton shower is comparable to the enhancement obtained from the reweighting procedure,

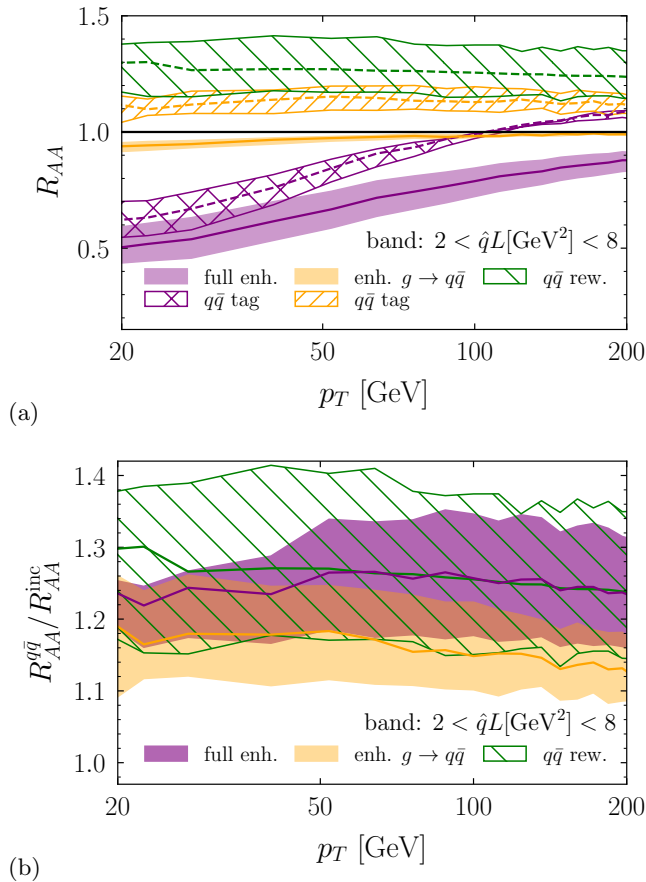


FIG. 2. (a) Results of the simplified stand-alone parton shower for the nuclear modification factor of inclusive (solid band) and of  $q\bar{q}$ -tagged (hatched band)  $R = 0.4$  jets. The case of BDMPS-Z medium-modifications to all splitting functions (purple) is compared to the case of including  $g \rightarrow q\bar{q}$  splitting function only (orange). Results of the reweighting procedure (??) are included (green). (b) The ratio of tagged over inclusive jet  $R_{AA}$ 's.

thus justifying the use of the latter in the main paper. Second, inclusion of medium-modified  $g \rightarrow gg$  and  $q \rightarrow qg$  splitting has a numerically small effect on the ratio  $R_{AA}^{q\bar{q}}/R_{AA}^{\text{inc}}$  (cf. Fig. 2(b)) although it affects the

nuclear modification factors  $R_{AA}^{\text{inc}}$  and  $R_{AA}^{q\bar{q}}$  significantly (cf. Fig. 2(a)). This supports our conclusion that the  $g \rightarrow q\bar{q}$ -induced enhancement of  $q\bar{q}$ -tagged jets can be identified as an enhancement of  $N_{D^0\bar{D}^0}/N_{\text{jets}}$  even in the presence of energy loss. It is also consistent with the conclusion reached in a different way in our **JetMed** study (see main text) that the enhanced  $c\bar{c}$ -radiation is not due to medium-enhanced  $g \rightarrow gg$  followed by vacuum splitting of  $g \rightarrow c\bar{c}$ , but that it is due to medium-enhanced  $g \rightarrow c\bar{c}$  splitting.

\* maximilian.attems@cern.ch  
 † jasmine.brewer@cern.ch  
 ‡ gian.michele.innocenti@cern.ch  
 § aleksas.mazeliauskas@cern.ch  
 ¶ sohyun.park@cern.ch  
 \*\* wilke.van.der.schee@cern.ch  
 †† gregory.soyez@ipht.fr  
 ††† urs.wiedemann@cern.ch

- [1] P. Caucal, E. Iancu, A. H. Mueller, and G. Soyez, *Phys. Rev. Lett.* **120**, 232001 (2018), arXiv:1801.09703 [hep-ph].
- [2] P. Caucal, E. Iancu, and G. Soyez, *JHEP* **10**, 273 (2019), arXiv:1907.04866 [hep-ph].
- [3] P. Caucal, E. Iancu, A. H. Mueller, and G. Soyez, *JHEP* **10**, 204 (2020), arXiv:2005.05852 [hep-ph].
- [4] P. Caucal, E. Iancu, and G. Soyez, *JHEP* **04**, 209 (2021), arXiv:2012.01457 [hep-ph].
- [5] Y. Mehtar-Tani and S. Schlichting, *JHEP* **09**, 144 (2018), arXiv:1807.06181 [hep-ph].
- [6] Y. L. Dokshitzer, V. A. Khoze, and S. I. Troian, *J. Phys. G* **17**, 1602 (1991).
- [7] S. Höche, in *Theoretical Advanced Study Institute in Elementary Particle Physics: Journeys Through the Precision Frontier: Amplitudes for Colliders* (2015) pp. 235–295, arXiv:1411.4085 [hep-ph].
- [8] S. Höche, “Introduction to Parton Shower and Matching,” (2019).
- [9] N. Armesto, L. Cunqueiro, and C. A. Salgado, *Eur. Phys. J. C* **63**, 679 (2009), arXiv:0907.1014 [hep-ph].
- [10] A. Huss, A. Kurkela, A. Mazeliauskas, R. Paatelainen, W. van der Schee, and U. A. Wiedemann, *Phys. Rev. C* **103**, 054903 (2021), arXiv:2007.13758 [hep-ph].